

Three-Dimensional Nonlinear Theory of the Free Electron Laser

P. Sprangle* and Cha-Mei Tang†
Naval Research Laboratory, Washington, D. C.

The present paper deals primarily with finite transverse dimensional effects and efficiency enhancement methods in a steady-state free electron laser (FEL) amplifier configuration. In particular we treat, using a comprehensive formalism, finite transverse dimensional effects associated with 1) the wiggler field, 2) the electron beam, and 3) the total radiation beam. Our formulation includes efficiency enhancement schemes such as spatially contouring the wiggler field as well as accelerating the electron beam. The relationship between these various enhancement schemes is discussed. Finally, a finite transverse dimension illustrative example of a 10.6 μ FEL with enhanced efficiency is given.

I. Introduction

NUMEROUS publications treating the free electron laser (FEL) mechanism using a one-dimensional analytic and numerical model have appeared in the literature.¹⁻¹³ In many of these papers the nonlinear evolution of the radiation field together with various efficiency enhancement schemes have been studied. As of the writing of this paper, three-dimensional effects in the FEL have received little attention in the literature.¹⁴ It is the purpose of this paper to present a general nonlinear three-dimensional formulation of the steady-state FEL amplifier configuration including the various efficiency improvement schemes.

The transverse effects associated with a static magnetic wiggler field introduces modifications in the electron dynamics. A physically realizable magnetic wiggler field has transverse spatial variations as well as an axial component of the magnetic field in order to satisfy $\nabla \times \mathbf{B}_w = \nabla \cdot \mathbf{B}_w = 0$. The physically realizable wiggler fields causes slow betatron oscillations, which result in an increase in the effective axial beam temperature. If the effective beam temperature is large, it will significantly reduce the fraction of electrons trapped in the ponderomotive potential buckets.

The effects of finite transverse dimensions of the radiation and electron beam are interrelated. The radiation beam can be considered to be a superposition of the input field and excited field. The input Gaussian radiation beam diffracts as it propagates through the interaction region; its amplitude and phase change as a function of axial position. The excited radiation beam suffers from both diffraction and refraction. The profile of the excited radiation beam is, in general, not Gaussian. The waist of the input field is typically somewhat greater than the electron beam radius, whereas the effective waist of the excited field is comparable to the radius of the electron beam and, hence, it diffracts more rapidly than the input field. In general, the potential exists for destructive interference between the two fields. This would result in a decrease in the depth of the ponderomotive potential wells and cause detrapping of the electrons. However, destructive interference, in the parameter regime which we consider, is not observed.

A number of efficiency enhancement schemes for the FEL have been identified.^{7,8,10,11} Improved efficiency can be achieved by any or all of the following methods: 1) con-

touring, spatially in the longitudinal direction, the amplitude and/or wavelength of the magnetic wiggler field; and 2) applying an external dc electric field. By applying one or more of these efficiency enhancement schemes, the phase of the electrons trapped in the ponderomotive wave can be adjusted so that electron kinetic energy is converted into radiation. Our formulation will include and show the equivalence of the enumerated enhancement schemes.

Our nonlinear analysis of the three-dimensional FEL steady-state amplifier problem will be divided into two parts. In the first part, the electron dynamics are evaluated in the presence of a generalized linearly polarized wiggler, dc electric field and radiation field. A generalized pendulum-like equation for the phase of the particles with respect to the radiation field is obtained. In the second part, the dynamics of the radiation field governed by the particle dynamics is determined. In the analysis it proves convenient to represent the total radiation field as the sum of input and excited fields. The analytic form for both components of the radiation are explicitly evaluated. The wiggler field has transverse spatial gradients as well as an amplitude and wavelength which is an arbitrary function of axial position. The infinitely long electron beam is assumed to be initially cold and tenuous enough so that space charge effects can be neglected. The inclusion of an initial beam temperature as well as space charge effects are straightforward additions to the present formalism and have been included in previous one-dimensional formalisms.^{7,8,10}

II. Particle Dynamics—Derivation of Phase Equation

Our model of the FEL configuration is shown in Fig. 1. We consider a linearly polarized magnetic wiggler field that is independent of x . The generalized linearly polarized wiggler and radiation field are represented by the following vector potentials.

$$A_w(y, z) = A_w(z) \cosh[k_w(z)y] \cos\left(\int_0^z k_w(z') dz'\right) \hat{e}_x \quad (1)$$

$$A_R(x, y, z, t) = A_R(x, y, z) \sin\left[\frac{\omega}{c} z - \omega t + \varphi(x, y, z)\right] \hat{e}_x \quad (2)$$

where $A_w(z)$ and $k_w(z) = 2\pi/l_w(z)$ are the slowly varying amplitude and wavenumber of the wiggler field, l_w is the wiggler wavelength, A_R and φ are the slowly varying amplitude and phase of the total radiation field, ω is the frequency of the radiation, and c is the speed of light.

We also include an external dc electric field $E_{dc}(z) = -\partial\phi_{dc}(z)/\partial z \hat{e}_z$. In all cases of interest $|A_w| \gg |A_R|$ by many orders of magnitude. Furthermore, it is necessary to have $k_w r_b \ll 1$ where r_b is the electron beam radius.⁴

Presented as Paper 80-1404 at the AIAA 13th Fluid and Plasma Dynamics Conference, Snowmass, Colo., July 14-16, 1980; submitted Sept. 19, 1980; revision received March 9, 1981. Copyright © American Institute of Aeronautics and Astronautics, Inc., 1980. All rights reserved.

*Head, Plasma Theory Branch of the Plasma Physics Division.

†Research Physicist, Plasma Theory Branch of the Plasma Physics Division.

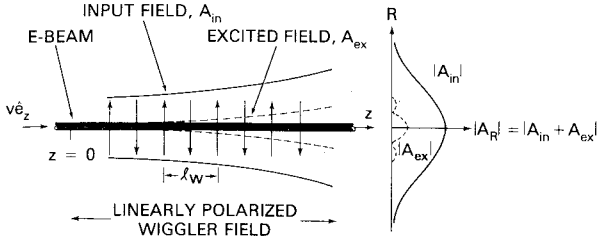


Fig. 1 Schematic of electron and radiation beams in three-dimensional FEL configuration.

Space charge effects will be neglected. This is appropriate if the beam density satisfies¹⁴

$$n_0 \ll (k_w^2 \gamma_{z0}^4 A_w A_R) (2\pi \gamma_0 m_0 c^2)^{-1} \quad (3)$$

where $\gamma_{z0} = (1 - v_{z0}^2/c^2)^{-1/2}$, v_{z0} is the axial velocity of the electron in the wiggler field, $\gamma_0 = (1 - v_0^2/c^2)^{-1/2}$, and v_0 is the magnitude of the total particle velocity. Equation (3) can be derived by comparing the ponderomotive term to the space charge term in the pendulum equation, see Ref. (12).

Electrons execute complicated trajectories in three dimensions. If radiation field, $A_R(x, y, z)$, varies little in the x direction over the electron beam, there is a constant of motion in the x direction.

$$P_x = \frac{|e|}{c} (A_w + A_R) \cdot \hat{e}_x \quad (4)$$

The particles in the y direction execute betatron type of orbits due to the gradient in the magnetic wiggler field. If a particle entered the interaction region $z=0$ with transverse coordinates (x_0, y_0) , and initial transverse velocity v_{y0} , the particle's transverse location at z is

$$\tilde{x} = x_0 + \frac{\beta_{0\perp}}{k_w} \cosh[k_w \tilde{y}] \sin \int_0^z k_w(z') dz' \quad (5a)$$

and

$$\tilde{y} = y_0 \cos K_0 z + (v_{y0}/K_0 v_{z0}) \sin K_0 z \quad (5b)$$

where $\beta_{0\perp} = v_{0\perp}/c$, $v_{0\perp} = |e| A_w / (\gamma_0 m_0 c)$ is the wiggler velocity, v_0 is the magnitude of total particle velocity and $K_0 = \beta_{0\perp} k_w / \sqrt{2}$.

The envelope of the electron beam in the y direction is not a constant in general. For example, if there is no initial transverse velocity spread in the y direction, i.e., $v_{y0}=0$, the electron beam undergoes periodic pinching in the y direction. All realizable electron beams have finite emittance. The emittance ϵ_y is defined as $\epsilon_y = \pi y_{0,\max} (v_{y0,\max}/c)$, where $y_{0,\max}$ and $v_{y0,\max}$ are the electron beam waist and the maximum velocity spread, respectively, in the y direction at the entrance of the magnetic wiggler. The condition for the envelope of the electron beam to remain approximately constant inside the wiggler with gradient is to require that the first and second terms on the right-hand side of Eq. (5b) be equal, i.e., $y_{0,\max} = v_{y0,\max} / (K_0 v_{z0}) = \sqrt{\epsilon_y / (\pi K_0)}$. The condition on $y_{0,\max}$ also leads to the smallest electron beam radius inside the wiggler field,

$$r_b = \sqrt{2\epsilon_y / \pi K_0} \quad (6a)$$

The gradient in the wiggler field will lead to an increase in the energy spread associated with the axial motion. Let us consider a cold electron beam with total energy $\gamma_0 m_0 c^2$. Since part of the energy is associated with the transverse motion, the axial velocity of a particle decreases as the amplitude of the betatron oscillation increases. The maximum axial velocity shear, due to the wiggler gradient, is given by $\Delta v_{\text{shear}} = c(\beta_{0\perp} k_w r_b / 2)^2$, while the corresponding longitudinal energy spread is $\Delta E_{\text{shear}} = \gamma_{z0}^2 \gamma_0 (\Delta v_{\text{shear}} / c) m_0 c^2$.

One efficiency enhancement approach is to initially trap a large fraction of the electrons in the ponderomotive potential wells and adiabatically extract kinetic energy from the particles. In order to trap a substantial fraction of the electrons, we require the trapping potential to be larger or at least comparable to the axial particle energy spread, i.e., $|e| \phi_{\text{trap}} > \Delta E_{\text{shear}}$. The initial depth of the trapping potential is $|e| \phi_{\text{trap}} / (\gamma_0 m_0 c^2) = 2\sqrt{2} \gamma_{z0} \beta_{0\perp} (A_R / A_w)^{1/2}$. Thus, the radius of the electron beam r_b is limited to

$$r_b < (\gamma_{z0} k_w)^{-1} \left(\frac{8\sqrt{2} \gamma_{z0}}{\beta_{0\perp}} \right)^{1/2} \left(\frac{A_R}{A_w} \right)^{1/4} \quad (6b)$$

The axial electron dynamics is most crucial in the FEL mechanism. With this in mind, we start with the equation of motion for the axial electron velocity, which can be written in the form

$$\begin{aligned} \frac{dv_z}{dt} = & \frac{|e|}{\gamma_z^2 \gamma m_0} \frac{\partial \phi_{\text{dc}}}{\partial z} - \frac{|e|^2}{2\gamma^2 m_0^2 c^2} \\ & \times \left[\frac{\partial}{\partial z} \left(A_w \cosh(k_w y) \cos \left(\int_0^z k_w dz' \right) \right)^2 \right. \\ & \left. + 2k_w A_w \cosh(k_w y) A_R \cos \left(\int_0^z \left(\frac{\omega}{c} + k_w \right) dz' - \omega t + \varphi \right) \right] \end{aligned} \quad (7)$$

where $v_z = v_z(x, y, z, t)$ is the axial electron velocity, $\gamma_z = (1 - v_z^2/c^2)^{-1/2}$, $\gamma = \gamma_z \gamma_{0\perp}$, $\gamma_{0\perp}(z) = [1 + (|e| A_w(z) / (m_0 c^2))^2]^{1/2}$. In obtaining Eq. (7) we have taken $\omega \approx \gamma_z^2 (1 + v_z/c) c k_w$ and the x component of electron momentum to be $(|e|/c)(A_w(y, z) + A_R(x, y, z, t)) \cdot \hat{e}_x$.

The second term on the right-hand side of Eq. (7) indicates that the axial velocity in a linearly polarized wiggler has an oscillatory component at twice the wiggler wavenumber. In Ref. 13 we showed that the axial oscillation is not large enough to cause particle detrapping in the ponderomotive potential well and, thus, it does not have a qualitative effect on the FEL mechanism.

At this point we perform a transformation^{7,8} from the Eulerian independent variables x, y, z, t , to Lagrangian independent variables $\tilde{z}, t_0, x_0, y_0, v_{y0}$ where t_0, x_0, y_0, v_{y0} are a particle's time, transverse coordinates, and transverse velocity at the entrance to the interaction region, i.e., $z=0$.

The equation governing the relative phase between the electrons and the ponderomotive wave (see Ref. 12 for one-dimensional derivation) is given by the generalized pendulum like equation

$$\begin{aligned} \frac{\partial^2 \tilde{\psi}}{\partial z^2} = & \frac{d^2 \varphi}{dz^2} + \frac{dk_w}{dz} + \frac{|e| \omega / c}{\tilde{\gamma}_z^2 \tilde{\gamma} m_0 c^2} \frac{\partial \phi_{\text{dc}}}{\partial z} \\ & - \frac{|e|^2 \omega / c}{2\tilde{\gamma}_z^2 m_0^2 c^4} \left[\frac{\partial}{\partial z} \left(A_w \cosh(k_w \tilde{y}) \cos \int_0^z k_w dz' \right)^2 \right. \\ & \left. + 2k_w A_w \cosh(k_w \tilde{y}) A_R(\tilde{x}, \tilde{y}, z) \cos \tilde{\psi} \right] \end{aligned} \quad (8)$$

where

$$\tilde{\psi} = \tilde{\psi}(z, t_0, x_0, y_0, v_{y0}) = \int_0^z (\omega/c + k_w(z')) dz' - \omega \tilde{t} + \varphi(\tilde{x}, \tilde{y}, z)$$

is the phase,

$$\tilde{t} = t_0 + \int_0^z \frac{dz'}{\tilde{v}_z}, \quad \tilde{\gamma} = \tilde{\gamma}_z \gamma_{0\perp}, \quad \tilde{\gamma}_z = (1 - \tilde{v}_z^2/c^2)^{-1/2}$$

$$\tilde{v}_z = \omega / (\omega/c + k_w(z) - \partial \tilde{\psi} / \partial z + d\varphi/dz)$$

is the electron axial velocity.

Equations (5) and (8) completely describe the nonlinear particle dynamics in terms of the fields A_w and A_R . Noting the structure of Eq. (8), it becomes clear that contouring the wiggler wavelength and/or amplitude, i.e., dk_w/dz or dA_w^2/dz , is directly equivalent to applying dc electric field, i.e., $\partial\phi_{dc}/\partial z$.

III. Evolution of Total Radiation Field

The radiation field satisfies the wave equation

$$(\nabla^2 - c^{-2}\partial^2/\partial t^2)A_R = -4\pi c^{-1}J_x \hat{e}_x \quad (9)$$

where the current density is given by

$$J_x(x, y, z, t) = -|e|n_0 v_0 \int_{-\infty}^{\infty} dt_0 \int_{-\infty}^{\infty} dx_0 \int_{-\infty}^{\infty} dy_0 \int_{-\infty}^{\infty} \times dv_{y0} \sigma(v_{y0}) \theta(x_0, y_0) \delta(x - \bar{x}) \delta(y - \bar{y}) \delta(t - \bar{t}) (\bar{P}_x / \bar{P}_z) \quad (10)$$

here $\theta(x_0, y_0)$ is a function which describes the initial electron beam profile, and $\sigma(v_{y0})$ is a function which describes the initial transverse velocity profile in y direction, n_0 is the constant electron beam density on axis prior to entering the interaction region, $\bar{P}_x \approx (|e|/c)A_w(\bar{y}, z) \cdot \hat{e}_x$ is the equilibrium particle momentum in the x direction, and $\bar{P}_z = \gamma m_0 \bar{v}_z$ is the axial particle momentum. The integrations in Eq. (10) are over all initial entrance times and transverse coordinates. We can solve for A_R using Fourier transform techniques.

The radiation field in Eq. (2) can be represented in the form

$$A_R(x, y, z, t) = (2i)^{-1} a(x, y, z) \exp(i\omega z/c - \omega t) \hat{e}_x + \text{c.c.} \quad (11)$$

where $a = A_R \exp(i\varphi)$ is the complex field amplitude and c.c. is the complex conjugate. A_R and φ are slowly varying functions of z . Substituting Eqs. (10) and (11) into the wave Eq. (9), and operating on it with

$$\int_0^{2\pi/\omega} dt \exp[-i(\omega z/c - \omega t)]$$

we obtain an equation for $a(x, y, z)$,

$$\left(\frac{\partial^2}{\partial x^2} + \frac{\partial^2}{\partial y^2} + 2i \frac{\omega}{c} \frac{\partial}{\partial z} \right) a(x, y, z) = j(x, y, z) \quad (12)$$

where

$$j(x, y, z) = i \frac{\omega_b^2}{c^2} \int_0^{2\pi/\omega} \frac{dt_0}{(2\pi/\omega)} \int_{-\infty}^{\infty} dx_0 \times \int_{-\infty}^{\infty} dy_0 \theta(x_0, y_0) \int_{-\infty}^{\infty} dv_{y0} \sigma(v_{y0}) \times \delta(x - \bar{x}) \delta(y - \bar{y}) \frac{A_w}{\bar{\gamma}} \cosh(k_w \bar{y}) \exp(-i(\bar{\psi} - \varphi)) \quad (13)$$

and $\omega_b = (4\pi |e|^2 n_0 / m_0)^{1/2}$. Denoting the multiple Fourier transform of $a(x, y, z)$ and $j(x, y, z)$ by $\hat{a}(k_x, k_y, z)$ and $\hat{j}(k_x, k_y, z)$, respectively, we can solve for $a(x, y, z)$ in Eq. (12) and arrive at

$$a(x, y, z) = \frac{1}{(2\pi)^2} \int_{-\infty}^{\infty} \int_{-\infty}^{\infty} \hat{a}(k_x, k_y, 0) \exp \left[i(k_x x + k_y y - \frac{k^2 z}{2\omega/c}) \right] dk_x dk_y - \frac{i}{2\omega/c} \frac{1}{(2\pi)^2} \int_0^z \int_{-\infty}^{\infty} \int_{-\infty}^{\infty} \times \hat{g}(k_x, k_y, z - z') \hat{j}(k_x, k_y, z') \exp[i(k_x x + k_y y)] dk_x dk_y dz' \quad (14)$$

where

$$\hat{g}(k_x, k_y, z - z') = \exp(-ik^2(z - z')/(2\omega/c)),$$

$$k^2 = k_x^2 + k_y^2$$

and

$$(a, j) = (2\pi)^{-2} \int_{-\infty}^{\infty} \int_{-\infty}^{\infty} (\hat{a}, \hat{j}) \exp[i(k_x x + k_y y)] dk_x dk_y$$

The first term on the right-hand side of Eq. (14) is the homogeneous solution of Eq. (12) and represents the input radiation field whereas the second term (driven solution) represents the excited radiation field. Taking the input field to be the lowest order Gaussian radiation beam we find

$$a_{in}(x, y, z) = A_{in}(w_0/w(z)) \exp\{-r^2/w^2(z) + i(r^2\omega/2R(z)c - \tan^{-1}(z/z_0))\} \quad (15)$$

where A_{in} is the amplitude of the input field, w_0 is the minimum waist, $w(z) = w_0(1 + (z/z_0)^2)^{1/2}$, $z_0 = w_0^2\omega/2c$ is the Rayleigh length of the input field and $R(z) = z(1 + (z/z_0)^2)$ is the radius of curvature of the wavefront. Noting that the excited field in Eq. (14) is in form of a convolution integral, it is possible to write it as

$$a_{ex}(x, y, z) = -\frac{i}{4\pi} \frac{\omega_b^2}{c^2} \int_0^z dz' \int_0^{2\pi/\omega} \frac{dt_0}{2\pi/\omega} \int_{-\infty}^{\infty} dx_0 \int_{-\infty}^{\infty} dy_0 \times \int_{-\infty}^{\infty} dv_{y0} \sigma(v_{y0}) \theta(x_0, y_0) \frac{A'_w}{\bar{\gamma}'} \cosh(k'_w \bar{y}') \frac{1}{z - z'} \times \exp \left[i((x - \bar{x}')^2 + (y - \bar{y}')^2) \frac{\omega/c}{2(z - z')} \right] \times \exp[-i(\bar{\psi}' - \varphi')] \quad (16)$$

where the primes on quantities denote functions of z' . Equations (5), (8), (15), and (16) describe self-consistently the nonlinear three-dimensional steady state FEL amplifier.

IV. Illustration of Three-Dimensional Effects

For purposes of illustrating transverse effects in the radiation field, we will consider a FEL having axial symmetry and operating in the low gain limit, i.e., $|a_{in}| \gg |a_{ex}|$. We chose a Gaussian electron beam profile, $\theta = \exp[-(x_0^2 + y_0^2)/r_b^2]$, where r_b is the radius of the electron beam. If r_b satisfies Eqs. (6a, b) and $k_w r_b \ll 1$, then we can neglect the gradient in the wiggler and replace, \bar{x} , \bar{y} in Eq. (16) by x_0 , y_0 , and $\sigma(v_{y0})$ by $\delta(v_{y0})$. For a low gain FEL and a plane wave input field a_{in} the phase $\bar{\psi}$ is very nearly a function of z and t_0 only. With these simplifying assumptions, Eq. (16) can be integrated to give

$$a_{ex}(r, z) = -\frac{i}{4} \frac{\omega_b^2/c^2}{\gamma_0} r_b^2 \int_0^{2\pi/\omega} \frac{dt_0}{2\pi/\omega} \int_0^z dz' A_w(z') e^{i\varphi(z')} \times \left(\frac{z - z' + iz_b}{(z - z')^2 + z_b^2} \right) \exp \left[-i(\bar{\psi}(z') - \varphi) - z_b \left(\frac{z - z' + iz_b}{(z - z')^2 + z_b^2} \right) \frac{r^2}{r_b^2} \right] \quad (17)$$

where $z_b = r_b^2\omega/2c$ is the effective Rayleigh length associated with the excited radiation.

A square or Lorentzian electron beam profile may also be readily integrated in Eq. (16). The one-dimensional limit of Eq. (17) is obtained by letting z_b or r_b approach ∞ .

We will now make the constant phase, resonant particle approximation. In this approximation all particles are assumed to have the same constant phase, $\bar{\psi}_R$. The electron beam in this approximation consists of a pulse train of macroparticles separated in distance by $2\pi v_{0z}/\omega$. Furthermore, we will limit ourselves at this point to a constant parameter wiggler and consider only an external dc electric potential. The rate of change, on axis, of the resonant particle energy is

$$\frac{\partial(\gamma_R m_0 c^2)}{\partial z} = |e| \frac{\partial \phi_{dc}(z)}{\partial z} - \frac{|e|^2 \omega/c}{2\gamma_R m_0 c^2} A_w A_R(r=0, z) \cos \bar{\psi}_R \quad (18)$$

where $\gamma_R = \gamma_R(r=0, z)$ is the relativistic factor for the resonant particle on axis. From Eq. (8), the constant resonant phase is found to be given by

$$\cos \bar{\psi}_R = \frac{(|e|(\omega/c) \partial \phi_{dc}/\partial z) / (\gamma_{zR}^2 \gamma_R m_0 c^2) + \partial^2 \varphi / \partial z^2}{|e|(\omega/c) k_w A_w A_R(z) / (\gamma_R^2 m_0^2 c^4)} \quad (19)$$

where the z dependence of $\partial \phi_{dc}/\partial z$ is such that $\cos \bar{\psi}_R$ is independent of z and γ_{zR} is the axial resonant relativistic factor on axis.

To obtain the total radiation field we first evaluate $a_{ex}(r, z)$ under the assumption that $|\varphi| \ll 1$. This will be shown later to be valid. The excited resonant particle radiation a_{ex} for all r and z is

$$a_{ex}(r, z) = -i\alpha_0^2 A_w \left[E_i \left(\frac{-r^2}{r_b^2} \right) - E_i \left(\frac{-r^2}{r_b^2} \frac{z_b^2 - iz_b z}{z_b^2 + z^2} \right) \right] \times \exp(-i\bar{\psi}_R) \quad (20)$$

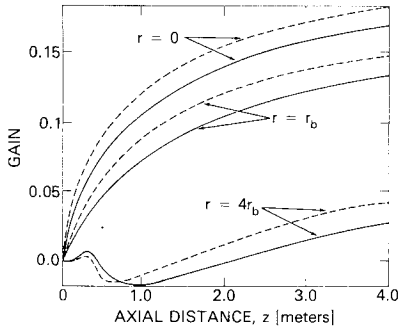


Fig. 2 Plots of gain as a function of axial position z at various radial positions for resonant macroparticles; the solid curves are for $\cos \bar{\psi}_R = 0$, and the dashed curves for $\cos \bar{\psi}_R = 0.3$.

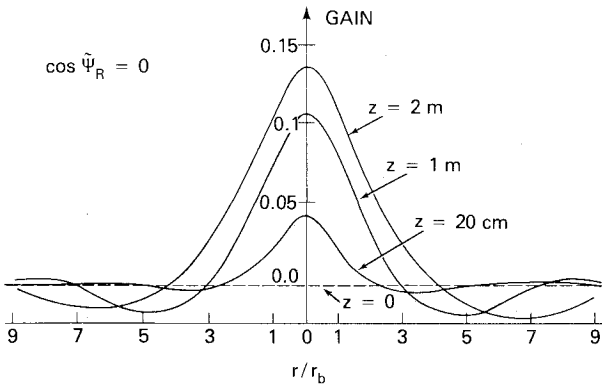


Fig. 3 Gain as a function of radius at $z = 20$ cm, 1 and 2 m for resonant macroparticles with $\cos \bar{\psi}_R = 0$.

where $\alpha_0 = \omega_b r_b / 2c\sqrt{\gamma_0}$ and E_i is the exponential integral function. The amplitude and phase of the total field, on axis $r=0$, are

$$A_R(r=0, z) = A_{in} + \alpha_0^2 A_w \left[\tan^{-1} \left(\frac{z}{z_b} \right) \cos \bar{\psi}_R - \ln \left(\frac{z^2 + z_b^2}{z_b^2} \right)^{1/2} \sin \bar{\psi}_R \right] \quad (21a)$$

$$\varphi(r=0, z) = -\alpha_0^2 (A_w / A_R) \left[\tan^{-1} \left(\frac{z}{z_b} \right) \sin \bar{\psi}_R + \ln \left(\frac{z^2 + z_b^2}{z_b^2} \right)^{1/2} \cos \bar{\psi}_R \right] \quad (21b)$$

where $A_{in} = |a_{in}|$, and stationary phase $\bar{\psi}_R$ is obtained from Eq. (8). We immediately notice that in the absence of an dc electric potential, i.e., $\phi_{dc} = 0$, the constant resonant phase $\bar{\psi}_R = -\pi/2$ is stationary, see Eq. (8), and results in a constant resonant particle energy, see Eq. (18). According to Eq. (21a), however, the total radiation field amplitude increases on axis and is given by

$$A_R(r=0, z) = A_{in} + \alpha_0^2 A_w \ln \left((z^2 + z_b^2) / z_b^2 \right)^{1/2}$$

The growth of the total radiation field on axis is due to refraction. The index of refraction, in this case, is greater than unity, $n = 1 + (c/\omega) \partial \varphi / \partial z > 1$ over the electron beam, hence the input field tends to focus while the electron beam will defocus. The net radiation energy flux along the z axis (integrated from $r=0$ to $r=\infty$) is constant, since for large r the radiation amplitude is less than the input amplitude.

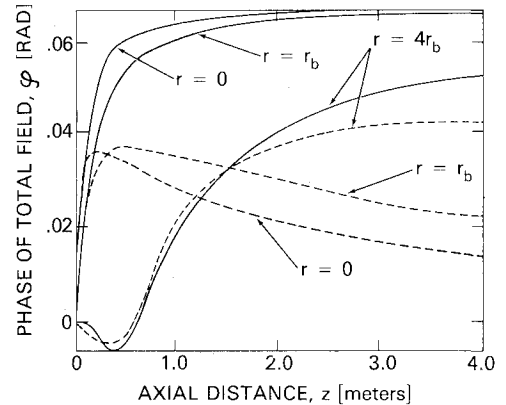


Fig. 4 Plots of total radiation phase φ as a function of axial position z at various radial positions for resonant macroparticles; the solid curves are for $\cos \bar{\psi}_R = 0$, and the dashed curves are for $\cos \bar{\psi}_R = 0.3$.

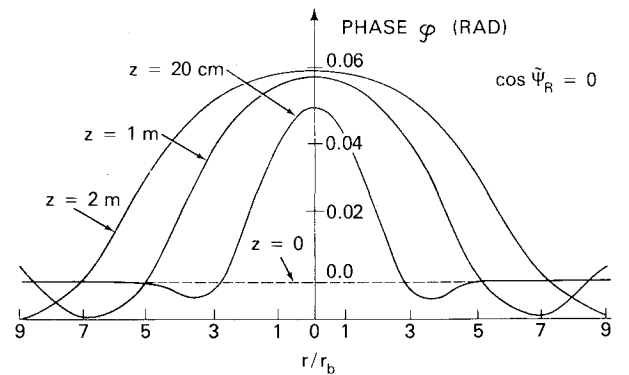


Fig. 5 Total radiation phase φ as a function of radius at $z = 20$ cm, 1 and 2 m for resonant macroparticles with $\cos \bar{\psi}_R = 0$.

V. Numerical Example

As an example of a 10.6 μm FEL utilizing a CO_2 laser as an input field, we chose an electron beam of energy 25 MeV ($\gamma_0 = 50$), current of $I = 5$ A and radius (Gaussian profile) of $r_b = 0.5$ mm. Such a beam has a peak density on axis of $n_0 = 1.3 \times 10^{11} \text{ cm}^{-3}$ ($\omega_b = 2.0 \times 10^{10} \text{ s}^{-1}$). The constant parameter wiggler has a magnitude of $B_w = 5.0$ kG and wavelength of $l_w = 2.8$ cm which gives $A_w = 2.2 \times 10^3$ statvolts. The wiggle velocity is $v_{0\perp} = 2.6 \times 10^{-2} c$ and the input CO_2 power density is taken to be $P_{\text{in}} = 4 \times 10^8 \text{ W/cm}^2$ which gives $A_{\text{in}} = 0.30$ statvolts. Note that the inequalities in Eqs. (3) and (6b) are well satisfied.

We make the resonant macroparticle approximation and obtain numerical results from Eq. (20). Our first illustration is one in which the applied dc electric potential is zero, hence, $\tilde{\psi}_R = -\pi/2$ and the particle energy remains constant. The solid curves in Fig. 2 show the gain,

$$G(r, z) = (A_R(r, z) - A_{\text{in}})/A_{\text{in}} \quad (22)$$

as a function of axial position z at various radial positions, i.e., $r=0$, $r=r_b$, and $r=4r_b$. The gain in the radiation amplitude at $z=2$ m is maximum on axis and equal to 0.14. Figure 3 shows the gain as a function of radius at $z=20$ cm, 1 and 2 m. The increase of radiation field on axis is at the expense of radiation field off axis.

The solid curves in Fig. 4 show the total radiation phase φ as a function of axial position at various radial positions. Figure 5 shows the radial cross section of total radiation phase φ at $z=20$ cm, 1 and 2 m. The maximum value of φ is along the z axis and is approximately 0.06 rad which certainly satisfies our approximation used in Eq. (18) to obtain Eq. (20). The index of refraction, in this case, is greater than unity, $n = 1 + (c/\omega) \partial \varphi / \partial z > 1$ over the electron beam.

Our next illustration still assumes resonant macroparticles, but will include an applied dc electric potential $\phi_{\text{dc}}(z)$ such that $\cos \tilde{\psi}_R = 0.3$. The dashed curves of Figs. 2 and 4 are the numerical results of Eq. (20) for this example. The gain in radiation amplitude on axis at $z=2$ m is 0.15, see Fig. 2. The dashed curves in Fig. 4 show the phase φ as a function of z . For large z , n is less than unity on axis (defocusing) and becomes greater than unity for large r (focusing).

The energy gained in propagating the electron beam through the potential ϕ_{dc} is converted into radiation energy. The efficiency therefore can be defined as

$$\begin{aligned} \eta &= |e| (\phi_{\text{dc}}(z) - \phi_{\text{dc}}(0)) / \gamma_0 m_0 c^2 \\ &\approx \pi (v_{0\perp} / c)^2 (A_{\text{in}} / A_w) (z / \lambda) \cos \tilde{\psi}_R \end{aligned} \quad (23)$$

where λ is the radiation wavelength. The efficiency is approximately a linear function of axial position and is $\sim 1.8\%$ at $z=2$ m.

Acknowledgment

The authors appreciate useful discussions with I. B. Bernstein and W. M. Manheimer. The authors would also like to acknowledge support for this work by DARPA under Contract 3817.

References

- 1 Madey, J. M. J., "Stimulated Emission of Bremsstrahlung in a Periodic Magnetic Field," *Journal of Applied Physics*, Vol. 42, April 1971, pp. 1906-1913.
- 2 Sprangle, P. and Granatstein, V. L., "Simulated Cyclotron Resonance Scattering and Production of Powerful Submillimeter Radiation," *Applied Physics Letters*, Vol. 25, Oct. 1974, pp. 377-379.
- 3 Colson, W. B., "Theory of a Free Electron Laser," *Physics Letters*, Vol. 59A, Nov. 1976, pp. 187-190.
- 4 Sprangle, P., Smith, R. A., and Granatstein, V. L., "Free Electron Lasers and Stimulated Scattering from Relativistic Electron Beams," Naval Research Laboratory, Washington, D. C., NRL Memo Rept. 3911, Dec. 1978; also *Infrared and Millimeter Waves*, edited by K. Button, Vol. 1, Academic Press, 1979.
- 5 Kroll, N. K. and McMullin, W. A., "Stimulated Emission from Relativistic Electrons Passing Through a Spatially Periodic Transverse Magnetic Field," *Physical Review*, Vol. 17A, Jan. 1978, pp. 300-308.
- 6 Sprangle, P. and Drobot, A. T., "Stimulated Backscattering from Relativistic Unmagnetized Electron Beams," *Journal of Applied Physics*, Vol. 50, April 1979, pp. 2652-2661.
- 7 Sprangle, P., Tang, C. M., and Manheimer, W. M., "Nonlinear Formulation and Efficiency Enhancement of Free-Electron Lasers," *Physical Review Letters*, Vol. 43, Dec. 1979, pp. 1932-1936.
- 8 Sprangle, P., Tang, C. M., and Manheimer, W. M., "Nonlinear Theory of Free-Electron Lasers and Efficiency Enhancement," *Physical Review*, Vol. 21A, Jan. 1980, pp. 302-318.
- 9 Sprangle, P. and Smith, R. A., "Theory of Free-Electron Lasers," *Physical Review*, Vol. 21A, Jan. 1980, pp. 293-301.
- 10 *Free-Electron Generators of Coherent Radiation, Physics of Quantum Electronics*, Vol. 7, edited by S. F. Jacobs, H. S. Pilloff, M. Sargent III, M. O. Scully and R. Spitzer, Addison-Wesley Publishing Company, Reading, Mass., 1980.
- 11 Kroll, N. M., Morton, P., and Rosenbluth, M., "Free Electron Lasers with Variable Parameter Wigglers," SRI International, Arlington, Va., Jason Tech. Rept. JSR-79-01, Jan. 1980.
- 12 Sprangle, P. and Tang, C. M., "Formulation of Non-Linear Free Electron Laser Dynamics with Space Charge Effects and Spatially Varying Wiggler," *Conference Digest of the Fourth International Conference on Infrared and Millimeter Waves and their Applications*, 1979, pp. 98-100.
- 13 Tang, C. M. and Sprangle, P., "Non-Linear Analysis of the Free Electron Laser Utilizing a Linear Wiggler Field," Naval Research Laboratory, Washington, D. C., NRL Memo Rept. 4354, 1980; accepted for publication in *Journal of Applied Physics*.
- 14 Sprangle, P. and Tang, C. M., "Three Dimensional Non-Linear Theory of the Free Electron Laser," Naval Research Laboratory, Washington, D. C., NRL Memo Rept. 4280, Sept. 1980.